Original Research

Estimating the modulatory effect of cadmium chloride on the genotoxicity and mutagenicity of silver nanoparticles in mice

H. R. H. Mohamed*

Zoology Department, Faculty of Science, Cairo University, Giza, Egypt

Abstract: Silver (Ag) nanoparticles (nano-Ag) are widely used because of their distinctive antimicrobial properties, but this widespread use increases Ag release into the environment along with many other pollutants such as heavy metals. Therefore, this study was undertaken to study the modulatory effect of cadmium chloride (CdCl$_2$) on the genotoxicity and mutagenicity of nano-Ag in mice liver, kidney and brain tissues. Co-injections of CdCl$_2$ (1.5 mg/kg) with nano-Ag (20, 41, or 82 mg/kg) resulted in significant elevations in both single and double DNA strand breaks that triggered higher apoptotic DNA damage, as revealed by the more fragmented appearance of genomic DNA and the significant increase in apoptotic fractions. Concurrent higher mutation incidence in the presenilin-1 and p53 genes was observed after CdCl$_2$ co-treatment than in nano-Ag-treated groups. Immuno-histochemical localization of p53 protein revealed the overexpression of the p53 gene and the histological examination showed diffusely degenerated, congested blood vessels and the infiltration of leukocytes in the liver, kidney, and brain tissues of the groups co-treated with nano-Ag and CdCl$_2$. Moreover, CdCl$_2$ co-injection with nano-Ag increased reactive oxygen species (ROS) generation, as revealed by increased malondialdehyde levels, decreased glutathione levels, and decreased superoxide dismutase and glutathione peroxidase activity, compared with those induced by nano-Ag particles alone. We concluded that CdCl$_2$ enhanced the nano-Ag-induced genotoxicity via increasing mutation incidence in p53 and presenilin-1 gene.

Key words: Ag nanoparticles; Genotoxicity; Mutagenicity; CdCl$_2$; p53 and presenilin genes.

Introduction

The remarkable evolution of nanoparticles applications due to their characteristic properties including small surface area, small size and high catalytic activity, increases the human exposure to nanoparticles as well as many pollutants. Therefore, the study of the effect of these pollutants on the genetic toxicity of nanoparticles is inevitable to understand the toxic interactions between nanoparticles and pollutants.

Because of the potent antibacterial, antifungal and antiviral properties, nano-Ag particles widely used in a wide range of products including cosmetics, clothes, air- freshener sprays, surgical instruments, wound dressings and bone prostheses in addition to their uses in food packing to increase product shelf life (1,2). Nano-Ag particles are also extensively used in the environment, for example in the disinfection of drinking water, anti-fouling of swimming pool (3-6) and in water-based paints as an antibacterial additive, as well as their uses in medicine as antitumor, anti-inflammatory antiviral and antibacterial (7-12) agent and also in the promotion the wound healing (13). All these uses and applications have therefore increased their hulman exposure and risks, which require the understanding of the genotoxicity in the presence of other pollutants.

It has been shown that nano-Ag particles are translocated by blood circulation and accumulate in several organs including liver, spleen, testis, kidney and even brain causing hepatotoxicity, renal toxicity and neuro-toxicity when administered orally, subcutaneously or via inhalation (14-17). However, contrasting results were obtained on the nano-Ag induced clastogenicity. No change were observed in the frequencies of micronuclei in the bone marrow cells of Sprague-Dawley rat which were treated with uncapped nano-Ag particles (18, 19) and in the bone marrow and liver cells of mice and zebra fish treated with the nano-Ag capped with starch, bovine serum albumin, polyvinyl alcohol and poly vinyl pyrrolidone (PVP) (20-22). Despite, no DNA strand breaks were observed using a standard Comet assay, a modified enzyme Comet assay showing DNA strand breaks in the liver cells of mice treated with PVP or silicon coated nano-Ag (23).

The nano-Ag particles have been shown to increase structural chromosomal aberrations and micronuclei frequencies in bone marrow cells of rats either injected intraperitoneally with doses of nano-Ag 1.2 and 4 mg/kg daily for 28 days (24) or orally administered nano-Ag at 5, 25, 50 or 100, mg/kg body weight once daily for five consecutive days (25). In fact, DNA damage induction by nano-Ag has been shown by increasing both the DNA single- and double-strand breaks levels in rats and mice (26-28) and the γ-H2AX (a marker for DNA double-strand breaks) levels in zebra fish orally administrated nano-Ag particles (29). A study of Ahamed et al., (30) also showed the nano-Ag induced genotoxicity as revealed by the significant elevations in p53 and p38

proteins in *Drosophila melanogaster* treated with nano-Ag coated with polysaccharide.

Nano-Ag induced teratogenicity was also reported in several studies by the observed congenital malformations, decreased fetus viability, apoptotic damage in mouse embryos at the blastocyst stage, decreased implantation frequency, and delays in post-implantation development of embryos (20,31-33). Furthermore, nano-Ag particles caused significant reductions in the sperm counts and elevated the sperm abnormalities incidence in mice (28,34) and rats Gromadzka-Ostrowska *et al.* (35).

With increasing the nanoparticles usage in a variety of industrial, food and medical products human subjected to nano-Ag particles as well as many pollutants in food, water, air etc. Cadmium (Cd) is one of the most toxic heavy metals as released from minerals refining, cigarette smoking and smelting that increasing its level and causing pollution of water, air, and soil thereby accumulated in human body through food chain or direct exposure to Cd contaminated environment causing accumulations of Cd in various organs and tissues (36-38).

This Cd exposure has many adverse effects on human health, including respiratory tract irritation, pulmonary edema, renal dysfunction, osteoporosis, anemia and cancer (37,39) in addition to the neurological disorders e.g. learning disabilities and hyperactivity in children (40) and olfactory dysfunction and neurobehavioral defects in attention, psychomotor speed, and memory in workers exposed to Cd (37). Moreover, Cd induced genotoxicity has been shown in several studies by the reported significant elevations in micro-nucleated polychromatic erythrocytes in both tibia bone marrow cells and rats peripheral blood cells (41) and the elevated chromosomal aberrations and sister chromatid exchanges levels in Cd-exposed cells (42,43).

All these illustrate the need to study the effect of $CdCl_2$ co-administration on the genotoxicity and mutagenicity of nano-Ag and elucidating the possible molecular mechanisms for effect in this study. Alkaline comet assay was done to detect both single and double strand breaks. Apoptotic DNA damage was assessed using neutral comet and laddered DNA fragmentation assays. On the other hand single strand conformational polymorphism (SSCP) analysis was done to screen mutations in both p53 and presenilin-1 genes while immuno-histochemical localization of p53 protein was done using immunohistochemistry technique. Finally histological examination and biochemical measurements of oxidative stress markers were carried out to shed more light on their mechanisms.

Materials and Methods

Animals

The purchased male mice from the animal house of National Organization for Drug Control and Research (NODCAR) were Swiss webster strain (30-35 gram) and aging 10-12 weeks. For acclimatization mice were kept in our animal house for seven days under standard dark/light cycle and supplied with standard diet pellets and water that were given *ad libitum*.

Chemicals

Both of nano-Ag particles and $CdCl_2$ were obtained from the sigma chemical company (Sigma chemical Co., St. Louis, MO, USA). First $CdCl_2$ was obtained in the form of white $CdCl_2$ powder and dissolved in deionized water to prepare the selected injected dose (1.5 mg/kg) in this study and represented 25% fraction of the computed 24 hours LD50 (5.98 mg/kg) in mice by the study of Ali (44). On the other hand, nano-Ag particles were purchased in the form of grey powder with size <100 nm, its purity 99.5% and contains polyvinylpyrrolidone (PVP) as a dispersant. nano-Ag particles were suspended in deionized distilled water to prepare the doses required to inject mice in both preliminary test to detect its LD50 and the remaining experiments.

Nano Ag particles characterizations
X-Ray Diffraction (XRD)

Using a charge coupled device diffractometer (XPERT-PRO, PANalytical, The Netherlands) the XRD patterns of Nano-Agwere detected and the Scherrer's relationship ($D = 0.9\ k/B\cos h$) was used to calculate their particle size, where k is the wavelength of Xray, B is the broadening of diffraction line measured as half of its maximum intensity in radians, and h is the Bragg's diffraction angle. The particle size of sample has been estimated from the line width of XRD peak.

Dynamics Laser Scattering (DLS)

Malvern Instrument Zetasizer Nano Series (Malvern Instruments, Westborough, MA) equipped with a He-Ne laser ($\lambda = 633$ nm, max 5 mW) was used to detect the agglomeration size and Zeta potential of Ag nanoparticles.

Transmission Electron Spectroscopy (TEM)

To detect the particles size and morphology in aqueous suspensions, nano Ag suspensions in Milli-Q water were ultra-sonicated at 40 W for about 25 min and placed a drop of this suspension on carbon-coated copper TEM grids, dried, and finally operated TEM (a Tecnai G20, Super twin, double tilt) at an accelerating voltage of 200 kV.

Determination of Ag LD50

In order to determine the starting acute dose, mice were injected intraperitoneally (i.p) with each of the nano Ag different doses 500, 1500, 2500, 3500, 4000 or 5000 mg/kg b.w and observed for the clinical signs of toxicity, body weight effects, mortality and monitoring the dead mice number during the first 24 hours. Using the computer software EPA probit analysis by aid of NCSS package software, version 10, the nano Ag lethal dose causing the death of 50% of the animals (LD50) was calculated and the three fractions (1/100, 1/50 and 1/25) of the calculated LD50 dose were estimated.

Treatment Schedule

In this study forty male mice were used and randomly dived into eight groups, five per each, as follow: negative control group injected i.p with dist. water (group 1) and treated groups injected i.p with either $CdCl_2$ at the dose level 1.5 mg/kg b.w (group 2) or each of the nano-Ag different fractions (1/100, 1/50 or 1/25) of the cal-

culated LD50 (groups 3, 4 and 5) separately or both of CdCl$_2$ and nano-Ag (groups 6, 7, and 8) then all groups were sacrificed after 24 hours of the last treatment and dissected to expose the desired organs in accordance with the Guidelines of the National Institute of Health (NIH).

Alkaline comet Assay

Both of single and double DNA strand breaks were detected in the liver, kidney and brain tissues using the alkaline comet assay (45). In brief; homogenized a small piece of tissue weighting about 50 mg gently into mincing solution, mixed 10 µl of suspension containing about 10,000 cells with 75 µl of 0.5% low melting point agarose (Sigma) and spread on slides coated with normal melting agarose (1%). Cells were lysed after solidification in cold lysis buffer (2.5-M NaCl, 100-mM EDTA, and 10-mM Tris, pH 10) with freshly added 10% DMSO and 1% Triton X-100 for 24 hours at 4°C in dark. To unwind DNA the slides were incubated in fresh alkaline buffer (300-mM NaOH and 1-mM EDTA, pH _ 13) for 25 min that electrophoresed for 25 min at 300 mA and 25 V (0.90 V/cm) and neutralized in 0.4-M Trizma base (pH 7.5). Finally, slides were fixed in 100% cold ethanol, air dried, and stored at room temperature until they were scored. Slides were imaged by simultaneous image capture and 50 cells stained with ethidium bromide at ×400 magnification were scored using Komet 5 image analysis software developed by Kinetic Imaging, Ltd (Liverpool, UK). Tail length, %tail DNA and tail moment were used as DNA damage endpoints.

Neutral comet assay

Apoptotic DNA damage in liver, kidney and brain tissues were estimated using the neutral comet assay (46,47) as follow: spread cell suspensions on slides, lysed and electrophoresed for 30 min at 24 V in 1× TAE buffer (90 mM Tris, 2 mM EDTA, 90 mM boric acid, pH 8.4) at 4 °C. finally slides were stained with ethidium bromide and scored one thousands cells per animal included non-apoptotic (cells have no or little DNA migration), apoptotic (cells form structures with large fan-like tails and small heads) and necrotic or heavily damaged (cells have a long, thin tail of fragmented DNA) cells numbers were scored in one thousands cells per animal. Apoptotic fraction (AF) was calculated by dividing the number of apoptotic cells (apoptotic or necrotic cells) on the total number of cells examined and results were expressed as percentage of fragmentation observed in the control group.

Laddered DNA fragmentation assay

Apoptotic DNA damage was further studied using laddered DNA fragmentation because DNA fragmentation is considered as one of the later steps in the apoptotic process. Using Sriram et al. (48) method: cells were lysed in TE lysis buffer containing 0.5% sodium dodecyl sulfate then added 0.5 mg/mL RNase A and incubated at 37°C for 1 h. Proteinase K (0.2 mg/mL) was finally added and incubated the samples at 50°C overnight. After that, electrophoresed the extracted DNA using Phenol extraction method and precipitation by 7.5 M ammonium acetate and isopropanol in 1% agarose gel at 70 V and visualized using a UV transiluminator and photographed.

Single strand conformational polymorphism analysis

Mutations in Presenilin-1 (exon 5) and p53 (exon 7) genes were screened in liver, kidney and brain tissues using highly sensitive single strand conformational polymorphism (SSCP) technique. The extracted genomic DNA using Gene JET Genomic DNA Purification kit (Thermo Scientific #K0721, #K0722) were amplified by polymerase chain (PCR) using the primer sequences sense 5-aatctacaccccattcacag-3 and antisense 5-gcccccaactctcccacc-3 to amplify presenilin-1 gene (20) and sense 5-GCCGGCTCTGAGTATAC-CACC-3; and antisense 5-CTGGAGTCTTCCAGTG-TGATG-3 to amplify exon 7 of p53 gene (49,50) in a PCR reaction mixture containing the genomic DNA (50 ng), forward and reverse primers (30 pmol) and master mix. Thermal Cycler (Programmable Thermal Cycler, PTC-100TM thermal cycler, Model 96; MJ Research, Inc.,Watertown,MA, USA) were used to perform PCR reaction by initial denaturation at 94°C for 3mins followed by 35 cycles of denaturation at 94°C for 30 s, annealing at 60°C for presenilin-1 and 62°C for p53 genes for 1min, extension at 72°C for 1min and final extension at 72°C for 10 mins to complete amplification. To ensure the amplification of desired genes, PCR products were electrophoresed on a 1.5% ethidium bromide-treated agarose gel (Sigma, UK) and visualized using UV trans-illuminator. Finally purified PCR products were mixed with denaturing-loading dye (95% formamide, 0.1% bromophenol blue, 0.1% Xylene cyanol FF and 0.5 ml 15% Ficoll) and TE buffer, then denatured them by heating at 94 _C for 7 min and chilled on ice for 10 min to prevent re-annealing (Gasser et al., 2006). Electrophoresed samples at 90 V for ~45 minute then stained with ethidium bromide and examined using a UV transilluminator and photograph.

Histopathological examination

To see the effect of nano-Ag induced toxicity in the presence of CdCl$_2$ on the histological architecture, histopathological examination of the liver, kidney and brain tissues of mice treated with the highest nano Ag dose (1/25 of the LD50) either alone or simultaneously with CdCl$_2$ (1.5 mg/kg) was done by fixing, dehydrating, and clearing tissues that subsequently infiltrated with molten paraffin wax, embedded, trimmed, and finally sectioned into thin slices (4-5 mm thickness) using microtome and stained with hematoxylin and eosin.

Immuno-histochemical analysis

Effect of CdCl$_2$ on the expression of p53 genes was investigated using immune-histochemical localization of p53 protein in liver, kidney and brain of mice treated only with the highest nano Ag dose (1/25 of the LD50) either alone or simultaneously with CdCl$_2$ (1.5 mg/kg). Briefly; rehydrated the paraffin sections in graded alcohols series after dewaxing them in xylene then antigen retrieval in Tris-EDTA buffer was heat induced and blocked the non-specific binding using 10% non-immune serum. Incubated the tissue sections for 2 hours in p53 antibody diluted 1:50 with TBS and in TBS without primary antibody for negative control. Hydrogen

peroxide (3%) were used to block the endogenous peroxidase activity of tissues (BioGenex, San Ramon, CA, USA). Finally, incubated the tissue sections with 100 μl horse radish peroxidase (HRP) labeled mouse secondary antibody with DAB chromogen, stained them with hematoxylin for counterstain and examined using light microscope for p53 accumulation that stained brown.

Oxidative stress markers measurements

The malondialdehyde (MDA) and reduced glutathione (GSH) levels and activities of superoxide dismutase (SOD) and glutathione peroxidase (Gpx) enzymes were biochemically estimated in the liver, kidney and brain tissues of all groups as markers of oxidative stress.

MDA Level

According to the method described by Ohkawa et al. (51) MDA level was estimated by reacting the thiobarbituric acid (TBA) with MDA at temperature of 95°C in acidic medium for 45 min forming TBA reactive product reading the resultant pink product absorbance spectrophotometrically at 534 nm. Results were expressed as nmol/g tissue used.

Reduced GSH Level

The GSH level was measured using Beutler et al. (52) method by reducing Ellman's reagent (5, 5′ dithio bis-(2-nitrbenzoic acid)) with GSH to form 1 mol of 2-nitro-5-mercaptobenzoic acid (yellow compound) per mol of GSH. The reduced chromogen is directly proportional to GSH concentration and its absorbance was determined at 405 nm. Results were expressed as mmol/g tissue used.

SOD Activity

Using Nishikimi et al. (53) method SOD activity was measured based on its ability to inhibit the phenazine methosulfate-mediated reduction of nitroblue tetrazolium dye and results were expressed as μ/g tissue used.

GPx Activity

The GPx activity was assessed using Paglia and Valentine (54) based on a reaction in which oxidized glutathione (GSSG) is produced upon reduction of peroxides, and is recycled to its reduced state by the enzyme GSH reductase. The oxidation of NADPH to $NADP^+$ is accompanied by a decrease in absorbance at 340 nm (A_{340}) providing a spectrophotometric means for monitoring GPx enzyme activity. The rate of decrease in the A_{340} is directly proportional to the GPx activity in the sample. Results were expressed as μ/g tissue.

Statistical analysis

All data were expressed as mean ± S.D. and were analyzed using the statistical software package (SPSS 21) software at the significance level <0.05. First independent sample t-test was done to test the differences between each treated group and the control group. Second One way analysis of variance (ANOVA) was also performed to test the effect of nano-Ag different doses on the tested parameters with or without $CdCl_2$.

Results

Characterization of nano-Ag particles

According to the published data in Mohamed (28) study, results of XRD analysis proved the crystallite properties of bought nano-Ag by the appearance of three characteristic peaks in the 44∘, 64.4∘, and 77∘ in the XRD analysis curve and their size has been found to be ranged from 21.3 to 27.7 nm by Debye Scherrer's formula. However, dynamic laser scattering (DLS) revealed the high agglomeration and aggregation capacity of nano-Ag particles in deionized dist. water by the reported zeta potential mean 9.35mV and the polydispersity index (PdI) 1 values. As a result, it has been conducting ultra-sonication of nano-Ag suspension and confirmed using TEM imaging the dispersed form of nano-Ag suspension with averaged size 57.4567 ± 9.77 nm and also the cubic morphology of nano-Ag particles.

Lethality of nano-Ag particles

Fatalities marks were observed on the mice injected i.p. with nano-Ag particles at different dose levels of 500, 1500, 2500, 3500, 4000 or 5000 mg/kg b.w. including weakness, decreased locomotor activity, convulsions, flatulence, and Hind limb paralysis. 24 hours, half of the lethal dose (LD50) of it was found to be 2056 mg/kg b.w. by the Probit analysis software. The three doses of nano-Ag 20, 41 and 82 mg / kg represents 1/100, 1/50 and 1/25 of the calculated LD50, respectively, were tested in this study.

Alkaline comet assay

Examples for the scored nuclei with various degrees of DNA damage were shown in Fig. 1. As shown in Table 1 a single i.p. injection of either $CdCl_2$ (1.5 mg / kg bw) or nano-Ag particles (20, 41 or 82 mg / kg bw) alone resulted in statistical significant elevations in the tail length, %DNA in tail and tail moment compared with the negative control values. Co-injection of $CdCl_2$ with nano-Ag particles caused a dramatic DNA damage revealed by the high statistically significant increases in tail length, %DNA in tail and tail moment compared with negative control (p<0.001) and compa-
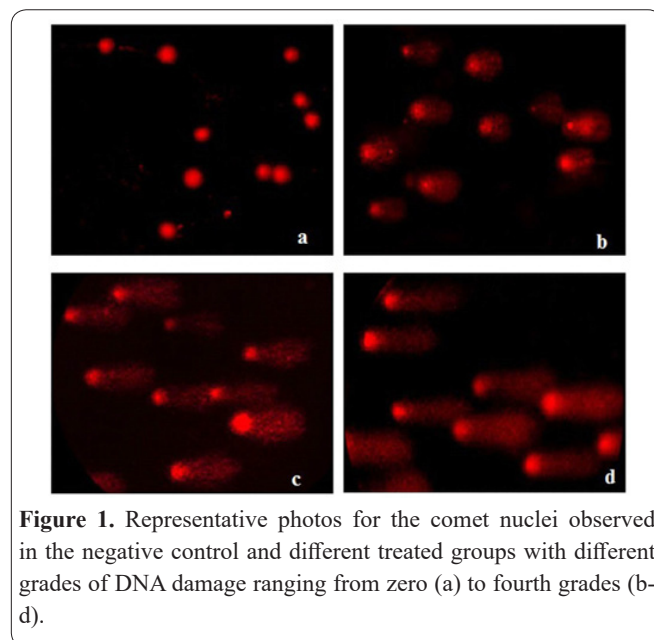
Figure 1. Representative photos for the comet nuclei observed in the negative control and different treated groups with different grades of DNA damage ranging from zero (a) to fourth grades (b-d).

Table 1. DNA damage level in mice groups injected i.p with nano-Ag particles different doses or $CdCl_2$ either separately or together simultaneously in liver (a), kidney (b) and brain (c) tissues.

a

Group	Treatment (mg/kg)	Tail length (px)	%DNA in tail	Tail moment
1	Negative control	4.95 ± 0.50	17.18 ± 1.70	1.08 ± 0.14
2	$Cd_{(1.5)}$	13.31 ± 1.81[a***]	25.31 ± 2.88[a***]	3.82 ± 0.97[a***]
3	$Ag_{(20)}$	14.73 ± 2.92[a***]	24.04 ± 1.57[a***]	3.64 ± 0.88[a***]
4	$Ag_{(41)}$	17.34 ± 3.82[a***]	26.55 ± 2.04[a***]	4.72 ± 0.68[a***]
5	$Ag_{(82)}$	22.28 ± 1.38[a***]	33.30 ± 2.03[a**]	7.43 ± 0.71[a***]
6	$Ag_{(20)}$+Cd	18.51 ± 0.70[a***,b*]	27.21 ± 1.34[a***,b*]	5.29 ± 0.56[a***,b**]
7	$Ag_{(41)}$+Cd	23.36 ± 3.11[a***,b*]	30.23 ± 2.56[a***,b*]	7.06 ± 0.94[a***,b**]
8	$Ag_{(82)}$+Cd	29.85 ± 1.57[a***,b***]	42.15 ± 3.14[a***,b**]	12.60 ± 0.79[a***,b***]
	Groups (3, 4 and 5)	F=8.81 p<0.01	F= 38.05 p< 0.001	F= 28.17 p<0.001
	Groups (6, 7 and 8)	F= 38.48 p<0.001	F=52.12 p<0.001	F=119.57 p<0.001

Results were expressed as mean ± S.D. [a]: statistically significantly different from the negative control group and [b]: statistically significantly different from the comparable nano-Ag treated group at p<0.05 [(*)], p<0.01 [(**)] and p<0.001[(***)] using student t-test. One way ANOVA was used to test the effect of different doses of nano-Ag particles on the tested parameters.

b

Group	Treatment (mg/kg)	Tail length (px)	%DNA in tail	Tail moment
1	Negative control	7.67 ± 1.09	19.62 ± 2.10	1.68 ± 0.42
2	$Cd_{(1.5)}$	19.14 ± 2.80[a***]	32.67 ± 3.83[a***]	6.46 ± 1.43[a***]
3	$Ag_{(20)}$	11.54 ± 1.52[a**]	25.79 ± 2.61[a**]	3.04 ± 0.66[a**]
4	$Ag_{(41)}$	21.01 ± 2.70[a***]	35.68 ± 2.02[a***]	7.80 ± 0.70[a***]
5	$Ag_{(82)}$	27.77 ± 1.90[a***]	42.21 ± 5.06[a**]	12.19 ± 1.45[a***]
6	$Ag_{(20)}$+Cd	20.41 ± 1.00[a***,b***]	31.58 ± 4.15[a***,b*]	6.49 ± 0.96[a***,b***]
7	$Ag_{(41)}$+Cd	26.56 ± 1.73[a***,b***]	43.99 ± 3.16[a***,b***]	11.74 ± 1.43[a***,b***]
8	$Ag_{(82)}$+Cd	34.74 ± 5.16[a***,b*]	55.31 ± 3.78[a***,b**]	19.41 ± 4.11[a***,b**]
	Groups (3, 4 and 5)	F=75.69 p<0.001	F= 28.10 p< 0.001	F= 102.98p<0.001
	Groups (6, 7 and 8)	F= 23.04p<0.001	F=50.85p<0.001	F=31.82p<0.001

Results were expressed as mean ± S.D. [a]: statistically significantly different from the negative control group and [b]: statistically significantly different from the comparable nano-Ag treated group at p<0.5 [(*)], p<0.01 [(**)] and p<0.001[(***)] using student t-test. One way ANOVA was used to test the effect of different doses of nano-Ag particles on the tested parameters.

c

Group	Treatment (mg/kg)	Tail length (px)	%DNA in tail	Tail moment
1	Negative control	6.45 ± 1.99	17.34 ± 1.64	1.50 ± 0.43
2	$Cd_{(1.5)}$	16.37 ± 2.10[a***]	30.96 ± 3.90[a***]	5.42 ± 2.03[a**]
3	$Ag_{(20)}$	13.00 ± 0.76[a***]	27.11 ± 4.54[a**]	3.71 ± 0.66[a**]
4	$Ag_{(41)}$	20.50 ± 4.19[a***]	36.21 ± 3.03[a***]	7.44 ± 1.74[a***]
5	$Ag_{(82)}$	25.70 ± 0.90[a***]	42.02 ± 4.33[a**]	10.79 ± 0.81[a***]
6	$Ag_{(20)}$+Cd	18.06 ± 2.96[a***,b**]	33.56 ± 2.90[a***,b*]	6.14 ± 1.44[a***,b**]
7	$Ag_{(41)}$+Cd	27.70 ± 1.21[a***,b**]	42.72 ± 2.34[a***,b**]	11.86 ± 1.00[a***,b**]
8	$Ag_{(82)}$+Cd	36.99 ± 5.54[a***,b***]	54.36 ± 2.95[a***,b**]	20.16 ± 2.52[a***,b***]
	Groups (3, 4 and 5)	F=32.23 p<0.001	F= 17.45p< 0.001	F= 45.09p<0.001
	Groups (6, 7 and 8)	F= 58.99p<0.001	F=72.13 p<0.001	F=78.82p<0.001

Results were expressed as mean ± S.D. [a]: statistically significantly different from the negative control group and [b]: statistically significantly different from the comparable nano-Ag treated group at p<0.5 [(*)], p<0.01 [(**)] and p<0.001[(***)] using student t-test. One way ANOVA was used to test the effect of different doses of nano-Ag particles on the tested parameters.

rable nano-Ag (p<0.05) treated groups. Moreover, one way ANOVA analysis confirmed the strong statistical dependence (p<0.001) of DNA damage parameters on nano-Ag doses in both groups treated with either nano-Ag particles alone or with $CdCl_2$ (Table 1a-c).

Neutral comet assay

Scoring of apoptotic and necrotic nuclei reflected the induction of apoptotic DNA damage in groups treated with $CdCl_2$ or nano-Ag either alone or simultaneously at the same time by the statistical significant elevations (p<0.001) in apoptotic fractions when compared with the negative control group (Table 2). Surprising, the apoptotic fraction was statistically significantly increased (p<0.05) in groups co-injected with $CdCl_2$ and nano-Ag particles compared with the comparable nano-Ag alone treated groups. Apoptotic fraction is heavily dependent on the dose of nano-Ag particles (p <0.001)

as shown by analysis of one way ANOVA in all groups treated with nano-Ag either alone or with $CdCl_2$ (Table 2).

Laddered DNA fragmentation

Apoptotic DNA fragmentation was increased obviously in the genomic DNA of groups injected simultaneously with both $CdCl_2$ (1.5 mg/kg) and each of nano-Ag three doses (20, 41 or 82 mg/kg) revealed by the fragmentized and smeared appearance compared with induced apoptotic DNA damage in nano-Ag treated groups liver, kidney and brain tissues (Fig. 2). However, lowest degree of apoptotic DNA was observed in the genomic DNA of brain tissues of all nano-Ag treated groups either alone or with $CdCl_2$. Also, $CdCl_2$ alone was induced apoptotic DNA damage in the genomic DNA of three tested tissues (Fig. 2).

Table 2. Apoptotic fraction in liver, kidney and brain tissues of mice injected i.p. with nano-Ag particles different doses and CdCl$_2$ either separately or together simultaneously.

Group	Treatment (mg/kg)	Apoptotic fraction (%)		
		Liver	Kidney	Brain
1	Negative control	3.50± 0.79	3.90 ± 0.65	3.80 ± 1.20
2	Cd$_{(1.5)}$	9.10± 0.89^{a***}	9.90 ± 1.74^{a***}	15.00 ± 2.55^{a***}
3	Ag$_{(20)}$	6.80 ± 0.91 ^{a***}	10.90 ± 1.56^{a***}	10.30 ± 1.79 ^{a***}
4	Ag$_{(41)}$	11.80 ± 1.52^{a***}	18.70± 1.60 ^{a***}	18.10 ± 1.60 ^{a***}
5	Ag$_{(82)}$	17.10 ± 1.88 ^{a***}	23.30 ± 2.51 ^{a***}	22.90 ± 3.89^{a***}
6	Ag$_{(20)}$+Cd	10.90 ± 1.08 ^{a***,b***}	15.10 ± 2.07 ^{a***,b**}	14.50 ± 2.24^{a***,b*}
7	Ag$_{(41)}$+Cd	16.10 ± 1.78 ^{a***,b**}	23.50 ± 2.45 ^{a***,b**}	22.20 ± 3.51^{a***,b*}
8	Ag$_{(82)}$+Cd	20.60± 2.58 ^{a***,b*}	27.40 ± 2.43^{a***,b*}	26.80 ± 3.01 ^{a***,b**}
Groups (3, 4 and 5)		F=59.40 p<0.001	F= 47.34p< 0.001	F= 28.99p<0.001
Groups (6, 7 and 8)		F= 32.06p<0.001	F=36.53 p<0.001	F=21.94p<0.001

Results were expressed as mean ± S.D. ^{a}: statistically significantly different from the negative control group and ^{b}: statistically significantly different from the comparable nano-Ag treated group at p<0.5 $^{(*)}$, p<0.01 $^{(**)}$ and p<0.001$^{(***)}$ using student t-test. One way ANOVA was used to test the effect of different doses of nano-Ag particles on the tested parameters.
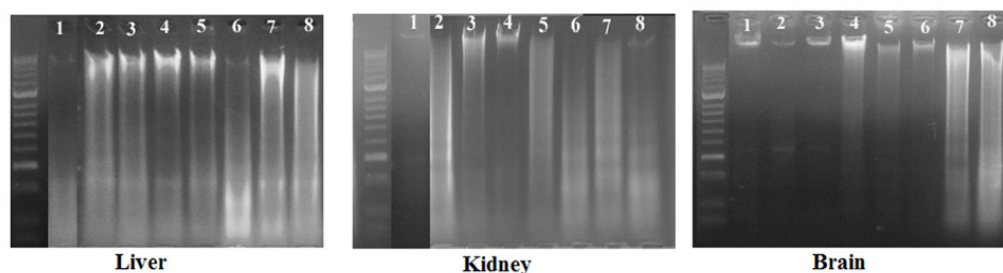
Figure 2. Pattern of the genomic DNA extracted from the negative control group (1) and groups injected i.p. with CdCl$_2$ (2) or different doses of nano-Ag particles (3-5) separately or simultaneously (6-8).
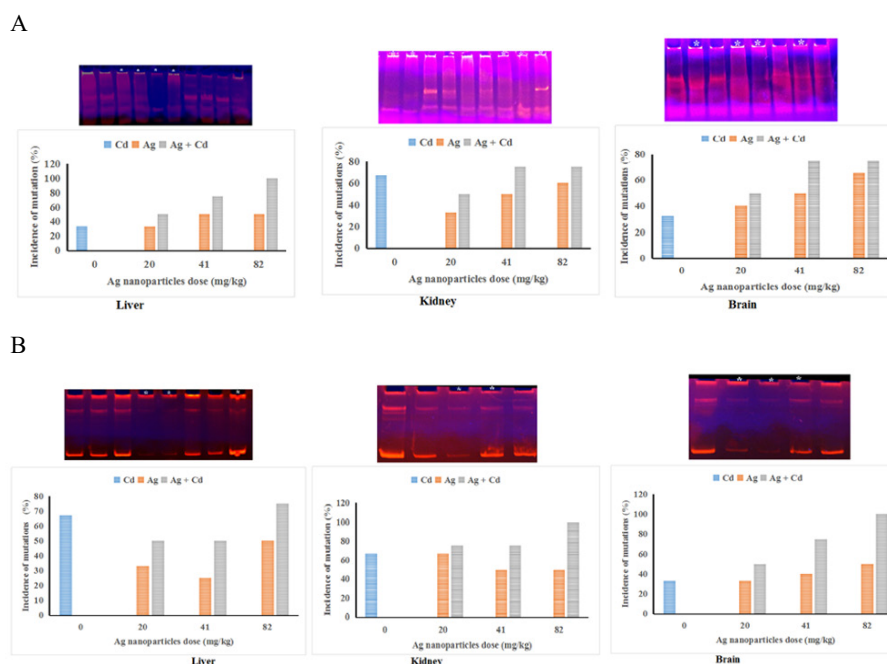
Figure 3. A: Incidence of mutations in the exon 7 of p53 gene of groups treated with nano-Ag (Ag) or/CdCl$_2$ (Cd): mutation in the representative photo was indicated by the symbol *. B: Incidence of mutations in the presenilin-1 gene of groups treated with nano-Ag (Ag) or/CdCl$_2$ (Cd): mutation in the representative photo was indicated by the symbol *.

Single strand conformational polymorphism (SSCP) analysis

Examination of mutations in the p53 and presenilin-1 genes using SSCP analysis demonstrated increased incidence of mutation in each of exon 7 of p53 gene and exon 5 of presenilin-1 gene after CdCl$_2$ co-injection with each of nano-Ag different doses compared to those resulting from the injection of each of the nano-Agthree different doses in the liver, kidney and brain testing organs (Fig. 3A &3B). Mutations have been observed in p53 and presenilin-1 gene also in mice injected with CdCl$_2$ alone and pointed to the different pattern of PCR products compared with the pattern of the negative control groups as shown in Fig. 3A & 3B. And the offered examples for mutations that have been observed in each of the p53 and presenilin genes are in Fig. 3.
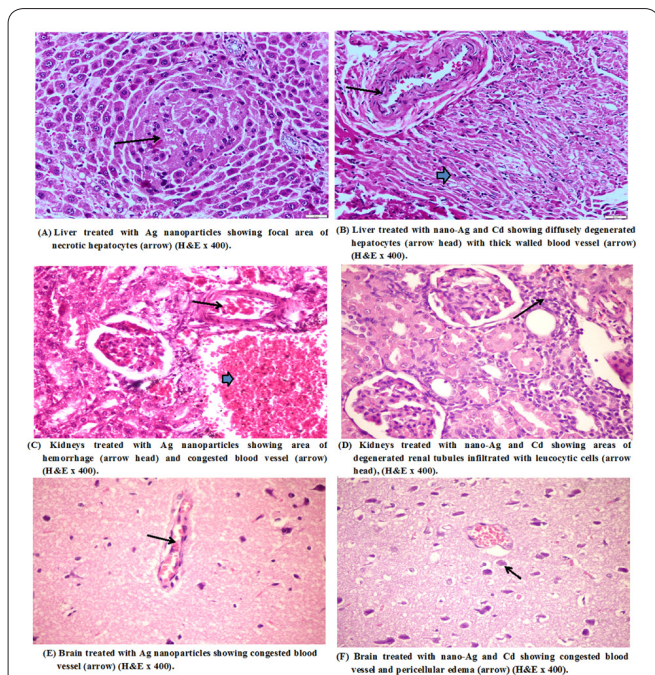
Figure 4. Histopathological examination of mice injected only with the highest dose of nano-Ag particles (82 mg/kg) either alone or simultaneously with CdCl$_2$.

Figure 5. Immuno-histochemical localization of p53 protein using Horse radish peroxidase labelled antibody: degree of expression is indicated by the symbol +.

treatment with nano-Ag alone (Fig. 5).

Histopathological examination

Histological examination showed focal area of necrotic hepatocytes in liver tissues, hemorrhage area in kidney tissues and congested blood vessel in both kidney and brain tissues of the group treated with nano-Ag particles (82 mg/kg) alone as shown in Fig. 4. In fact, CdCl$_2$ co-injection increased and multiplied these histological injuries as reflected by the observed diffusely degenerated hepatocytes with thick walled blood vessel, areas of degenerated renal tubules infiltrated with leucocytic cells and finally congested blood vessel and peri-cellular edema in the brain tissues (Fig. 4).

Immuno-histochemical localization of p53

Immuno-histochemical localization of p53 protein showed overexpression of p53 protein in group co-treated with CdCl$_2$ at 1.5 mg/kg and nano-Ag particles at 82 mg/kg by the emergence of a more intense and distribution of reddish brown color in the liver, kidney and brain tissues compared with that group that received

Oxidative stress biochemical markers

Single i.p. injections of either CdCl$_2$ at the dose level 1.5 mg/kg or each of the different nano-Ag 20, 41 or 82 mg/kg separately or even together simultaneously resulted in statistical significant elevations in the MDA level compared with that of the negative control (p<0.001) and comparable nano-Ag groups (p<0.05), respectively as shown in table 2. Dependence of MDA level on the doses nano-Ag doses in the nano-Ag treated groups either alone or with CdCl$_2$ was reflected by one way ANOVA analysis (p<0.001) (Table 3).

On contrary, the level of GSH protein and activities of Gpx and SOD enzymes were statistically significantly decreased in the groups that were injected i.p. either with CdCl$_2$ or each of the nano-Ag different doses compared with the negative control group. These antioxidants also were significantly dropped after CdCl$_2$ co-injection with each of the three different nano-Ag doses compared with the comparable nano-Ag treated group (Table 4-6). Moreover, the GSH level and Gpx and SOD

Table 3. Malondialdehyde (MDA) level in the liver, kidney and brain tissues of mice injected i.p. with nano-Ag particles different doses and CdCl$_2$ either separately or simultaneously.

Group	Treatment (mg/kg)	MDA level (nmol/g tissue)		
		Liver	**Kidney**	**Brain**
1	Negative control	38.45 ± 4.07	42.20 ± 8.17	32.40 ± 5.32
2	Cd$_{(1.5)}$	126.20 ± 11.19[a***]	163.50 ± 17.42[a***]	151.60 ± 10.97[a***]
3	Ag$_{(20)}$	95.40 ± 8.44 [a***]	88.00 ± 7.11[a***]	80.84 ± 7.02 [a***]
4	Ag$_{(41)}$	140.40 ± 8.50[a***]	124.20 ± 10.89 [a***]	123.60 ± 12.72 [a***]
5	Ag$_{(82)}$	164.80 ± 6.72 [a***]	159.40 ± 10.45 [a***]	160.20 ± 11.17[a***]
6	Ag$_{(20)}$+Cd	14.20 ± 9.28 [a***,b**]	135.27 ± 4.84[a***,b***]	117.80 ± 4.71[a***,b***]
7	Ag$_{(41)}$+Cd	155.00 ± 18.56 [a***]	167.40 ± 13.16 [a***,b***]	141.20 ± 9.36[a***,b*]
8	Ag$_{(82)}$+Cd	191.60 ± 15.44 [a***,b**]	203.00 ± 11.85[a***,b***]	180.80 ± 11.05 [a***,b*]
	Groups (3, 4 and 5)	F=98.74 p<0.001	F= 68.64p< 0.001	F= 70.45p<0.001
	Groups (6, 7 and 8)	F= 33.61p<0.001	F=51.05 p<0.001	F=65.54p<0.001

Results were expressed as mean ± S.D. [a]: statistically significantly different from the negative control group and [b]: statistically significantly different from the comparable nano-Ag treated group at p<0.5 [(*)], p<0.01 [(**)] and p<0.001[(***)] using student t-test. One way ANOVA was used to test the effect of different doses of nano-Ag particles on the tested parameters.

Table 4. Reduced glutathione (GSH) level in the liver, kidney and brain tissues of mice injected i.p. with nano-Ag particles different doses and $CdCl_2$ either separately or simultaneously.

Group	Treatment (mg/kg)	GSH level (µmol/g tissue)		
		Liver	Kidney	Brain
1	Negative control	0.506 ± 0.001	0.288 ± 0.003	0.257 ± 0.005
2	$Cd_{(1.5)}$	$0.271 \pm 0.007^{a***}$	$0.216 \pm 0.009^{a***}$	$0.177 \pm 0.003^{a***}$
3	$Ag_{(20)}$	$0.275 \pm 0.009^{a***}$	$0.178 \pm 0.007^{a***}$	$0.186 \pm 0.004^{a***}$
4	$Ag_{(41)}$	$0.193 \pm 0.004^{a***}$	$0.128 \pm 0.005^{a***}$	$0.137 \pm 0.006^{a***}$
5	$Ag_{(82)}$	$0.135 \pm 0.004^{a***}$	$0.095 \pm 0.007^{a***}$	$0.100 \pm 0.007^{a***}$
6	$Ag_{(20)}$+Cd	$0.176 \pm 0.008^{a***,b***}$	$0.147 \pm 0.006^{a***,b***}$	$0.149 \pm 0.008^{a***,b***}$
7	$Ag_{(41)}$+Cd	$0.120 \pm 0.009^{a***,b***}$	$0.099 \pm 0.007^{a***,b***}$	$0.113 \pm 0.004^{a***,b***}$
8	$Ag_{(82)}$+Cd	$0.081 \pm 0.007^{a***,b***}$	$0.057 \pm 0.006^{a***,b***}$	$0.079 \pm 0.006^{a***,b**}$
	Groups (3, 4 and 5)	F=632.20 p<0.001	F= 191.52p< 0.001	F= 288.73 p<0.001
	Groups (6, 7 and 8)	F= 169.18 p<0.001	F=255.52 p<0.001	F=147.05 p<0.001

Results were expressed as mean ± S.D. [a]: statistically significantly different from the negative control group and [b]: statistically significantly different from the comparable nano-Ag treated group at p<0.01 (**) and p<0.001(***) using student t-test. One way ANOVA was used to test the effect of different doses of nano-Ag particles on the tested parameters.

Table 5. Superoxide dismutase (SOD) activity in liver, kidney and brain tissues of mice injected i.p. with nano-Ag particles different doses and CdCl2 either separately or together simultaneously.

Group	Treatment (mg/kg)	SOD activity (U/g tissue)		
		Liver	Kidney	Brain
1	Negative control	7.61 ± 1.07	4.60 ± 0.97	10.34 ± 1.58
2	$Cd_{(1.5)}$	$3.83 \pm 0.99^{a***}$	$2.71 \pm 0.82^{a*}$	$7.77 \pm 1.29^{a*}$
3	$Ag_{(20)}$	$5.51 \pm 0.79^{a**}$	$3.20 \pm 0.90^{a*}$	$7.00 \pm 0.83^{a**}$
4	$Ag_{(41)}$	$4.06 \pm 0.72^{a***}$	$2.32 \pm 0.38^{a**}$	$5.40 \pm 0.96^{a**}$
5	$Ag_{(82)}$	$3.90 \pm 0.74^{a***}$	$1.91 \pm 0.46^{a**}$	$3.82 \pm 0.54^{a***}$
6	$Ag_{(20)}$+Cd	$3.58 \pm 0.68^{a***,b***}$	$2.68 \pm 0.69^{a**,b*}$	$6.08 \pm 0.75^{a**,b*}$
7	$Ag_{(41)}$+Cd	$3.00 \pm 0.79^{a***,b*}$	$1.72 \pm 0.38^{a***,b*}$	$4.46 \pm 0.69^{a***,b*}$
8	$Ag_{(82)}$+Cd	$1.73 \pm 0.58^{a***,b**}$	$1.07 \pm 0.28^{a***,b**}$	$2.66 \pm 0.59^{a***,b*}$
	Groups (3, 4 and 5)	F=6.99 p<0.05	F= 5.53 p< 0.05	F= 12.61 p<0.001
	Groups (6, 7 and 8)	F= 9.50 p<0.01	F=13.98 p<0.001	F=31.72 p<0.001

Results were expressed as mean ± S.D. [a]: statistically significantly different from the negative control group and [b]: statistically significantly different from the comparable nano-Ag treated group at p<0.05 (*), p<0.01 (**) and p<0.001(***) using student t-test. One way ANOVA was used to test the effect of different doses of nano-Ag particles on the tested parameters.

Table 6. Glutathione peroxidase (Gpx) activity in the liver, kidney and brain tissues of mice injected i.p. with nano-Ag particles different doses and $CdCl_2$ either separately or simultaneously.

Group	Treatment (mg/kg)	Gpx activity (U/g tissue)		
		Liver	Kidney	Brain
1	Negative control	173.60 ± 5.59	307.94 ± 16.80	206.80 ± 9.26
2	$Cd_{(1.5)}$	$81.36 \pm 8.07^{a***}$	$89.16 \pm 10.13^{a***}$	$98.80 \pm 7.85^{a***}$
3	$Ag_{(20)}$	$120.20 \pm 8.50^{a***}$	$199.60 \pm 12.50^{a***}$	$140.00 \pm 24.07^{a***}$
4	$Ag_{(41)}$	$77.16 \pm 7.91^{a***}$	$103.20 \pm 11.99^{a***}$	$80.80 \pm 8.23^{a***}$
5	$Ag_{(82)}$	$57.87 \pm 5.94^{a***}$	$66.40 \pm 7.44^{a***}$	$59.00 \pm 4.36^{a***}$
6	$Ag_{(20)}$+Cd	$90.05 \pm 3.84^{a***,b***}$	$84.80 \pm 5.89^{a***,b*}$	$78.40 \pm 6.65^{a***,b*}$
7	$Ag_{(41)}$+Cd	$58.60 \pm 9.02^{a***,b*}$	$54.80 \pm 8.40^{a***,b*}$	$50.00 \pm 7.90^{a***,b*}$
8	$Ag_{(82)}$+Cd	$40.98 \pm 6.37^{a***,b**}$	$36.00 \pm 6.36^{a***,b**}$	$23.40 \pm 5.59^{a***,b*}$
	Groups (3, 4 and 5)	F=89.79 p<0.001	F= 199.76 p< 0.001	F= 39.56 p<0.001
	Groups (6, 7 and 8)	F= 67.82 p<0.001	F=62.28 p<0.001	F=82.17 p<0.001

Results were expressed as mean ± S.D. [a]: statistically significantly different from the negative control group and [b]: statistically significantly different from the comparable nano-Ag treated group at p<0.05 (*), p<0.01 (**) and p<0.001(***) using student t-test. One way ANOVA was used to test the effect of different doses of nano-Ag particles on the tested parameters.

activities were significantly altered by changing the nano-Ag doses.

Discussion

Human exposure to a lot of pollutants in addition to a wide range of heavily used nanoparticles in the air, water, and food requires the study of toxic effects of nanoparticles in the presence of other pollutants. Serious impact of heavy metal Cd on life as industrial and agri-cultural practices increasing its level in the environment and deposition in various organs, for example through food containing dietary Cd intake (55,56), making the study of the effect of $CdCl_2$ on the toxic effects of the extensively used nano-Ag essential.

Because liver and kidney are target organs for accumulation of nano-Ag and also brain due to its ability to cross blood brain barrier reaching brain (57,58). The genotoxic effects of nano-Ag particles in the presence of $CdCl_2$ were studied in the liver, kidney and brain tissues

of mice in the current study.

Nano-Ag induced single and double strand breaks were dramatically enhanced by CdCl$_2$co-injection as evidenced by the by the significant increase in tail length, %DNA in tail and tail moment compared with those resulting from the injection of nano-Ag particles alone in the three examined organs liver, kidney and brain. Moreover, DNA damage inductions by either CdCl$_2$ or nano-Ag injected separately has been shown in several previous studies using alkaline comet assay (26-28,59-61) in a line with the significant increase observed in the DNA damage levels in liver, kidney and brain tissues.

Oxidative stress is considered as a main mechanism of DNA damage induction via generation of reactive oxygen species (ROS) that interact with lipid, protein and even with DNA producing single and double DNA strand breaks (62). Our finding of significant elevations in the MDA level and significant decreases in the antioxidant GSH level and the activities of Gpx and SOD enzymes after CdCl$_2$ co-injection first confirmed oxidative stress inductions by either nano-Ag different doses or CdCl$_2$ and also explained the enhancement of nano-Ag induced single and double strand DNA breaks by CdCl$_2$ co-treatment. Oxidative stress induction by CdCl$_2$ due to the release of Cd ions which replace copper and iron in various cytoplasmic and membrane proteins including ferritin and apoferritin resulting in elevations in the amount of free copper and iron ions thereby weakened cells, decreased their resistance, and increased their sensitivity to nano-Ag induced DNA damage (63,64).

As a result, CdCl$_2$ co-treatment reinforced the nano-Ag induced apoptotic DNA damage as shown by the significant elevations observed in apoptotic fraction and increased fragmentation of genomic DNA compared with those observed in groups treated with nano-Ag alone in agreement with the previous studies that have proven that single DNA strand breaks act as signals to induce apoptosis and double strand breaks trigger the apoptotic DNA damage (65-67). Double strand DNA breaks are one of the most serious and lethal types of DNA damage because a single DSB is sufficient to kill a cell or disturb its genomic integrity (68) and also these breaks resulting in chromosomal aberration, mitotic homologous recombination and mutation (69,70).

Almost all previous studies were focused on the role of presenilin-1 gene in the Alzheimer's disease pathogenesis since its discovery in 1995 but recently presenilin-1 mRNA has been shown to found abundantly in the peripheral tissues including liver, kidney, testis and spleen that are not affected in Alzheimer's disease (71,72). Therefore, mutations were screened in this study as an attempt to understand whether presenilin-1 gene has role in the toxic interaction between CdCl$_2$ and nano-Ag or not.

Surprising, mutations have been observed in the gene presenilin-1 in the tissues of liver, kidney and brain of animals treated with any nano-Ag doses or CdCl$_2$ separately and the high incidence of mutations in the gene presenilin-1 in the groups co-injected with each of different nano-Ag doses and CdCl$_2$ at one time compared with those observed in the nano-Ag treated groups. Presenilin-1 gene encoded Presenilin-1 protein, a ubiquitously expressed multi-transmembrane domain protein,

which is located primarily on the endoplasmic reticulum (ER), the Golgi apparatus, and plasma membrane function as a basic catalytic subunit for the γ-secretase complex involved in in the splitting of many of the first type transmembrane proteins, including β-amyloid β-amyloid precursor protein, Notch, CD44, Vascular Endothelial Growth Factor Receptor, E-cadherin and N-cadherin (73-76). Thus, the mutant presenilin-1 gene disrupted beta amyloid processing from its precursor and causing high rates of accumulation of beta-amyloid in the liver, kidney and brain of groups injected simultaneously with CdCl$_2$ and nano-Ag as presenilin-1 mutations caused perturbing the relative ratio between beta amyloid species and impairing developmental and cellular signaling pathways controlled by c-secretase substrates (77).

This accumulation of beta amyloid protein as recently shown not only give rise to Alzheimer's disease but also activate the p53 dependent apoptosis via p53 promotor (78,79). The findings of a high mutation incidence in exon 7 of p53 gene after CdCl$_2$ co-injection evidenced the influence of presenilin-1 gene mutations in the toxic interaction between nano-Ag and CdCl$_2$ via increased beta amyloid protein that caused disturbance in p53 sequence thereby alter its expression and increased p53 dependent apoptosis.

Histochemical localization of p53 protein in our study revealed its overexpression by CdCl$_2$ co-treatment in liver, kidney and brain in consistence with the previous study of Dorszewska and his colleagues (80) that showed that mutations in p53 exon 7 led to overexpression of p53 protein thereby increasing degenerative process. This increase in the degenerative process by CdCl$_2$ co-injection with nano-Ag is evident from the increase in histological injuries observed including: diffusely degenerated hepatocytes with thick walled blood vessel, areas of degenerated renal tubules infiltrated with leucocytic cells and finally congested blood vessel and pericellular edema in the brain tissues after CdCl$_2$ co-injection compared with the focal area of necrotic hepatocytes, hemorrhage area in kidney tissues and congested blood vessel in both kidney and brain tissues from the group that received treatment with nano-Ag particles (82 mg / kg) alone.

Hence co-administration of the heavy metal CdCl$_2$with nano-Ag increasing nano-Ag induced single and double DNA strand breaks that triggered and enhanced the induced apoptotic DNA damage via increasing MDA production and declined the antioxidants efficacy thereby weakened cells and increased mutation incidence in presenilin-1 and p53 genes. Therefore, more studies are recommended for further understanding of the effects of other pollutants on nano-Ag induced toxicity.

Conflict of interest
Author declared no conflict of interest.

Author's contributions
Author has all efforts and contribution in this manuscript.

References

1. Gottesman R, Shukla S, Perkas N, Solovyov LA, Nitzan Y, Ge-

danken A. Sonochemical coating of paper by microbiocidal silver nanoparticles. Langmuir 2011; 27: 720–726.

2. Ribeiro M, Morgado P, Miguel S, Coutinho P, Correia I. Dextran-based hydrogel containing chitosan microparticles loaded with growth factors to be used in wound healing. Mater Sci Eng 2013; 33:2958–2966

3. Li Q, Mahendra S, Lyon DY, Brunet L, Liga MV, Li D. Antimicrobial nanoma-terials for water disinfection and microbial control: potential applications and implications. Water Res 2008; 42:4591–602.

4. Lv Y, Liu H, Wang Z, Liu S, Hao L, Sang Y. Silver nanoparticle-decorated porous ceramic composite for water treatment. J Membr Sci 2009; 331: 50–6.

5. Yang HL, Lin JC, Huang C. Application of nanosilver surface modification to RO membrane and spacer for mitigating biofouling in seawater desalination? Water Res 2009; 43(15):3777–86.

6. Holtz RD, Lima BA, Souza, Filho AG, Brocchi M, Alves OL. Nanostructured silver vanadate as a promising antibacterial additive to water-based paints. Nanomed: Nanotechnol, Biol Med 2012; 6: 935–40.

7. Salata O. Application of nanoparticles in biology and medicine. J Nanobiotechnol 2004; 2:1-6.

8. Chen J, Choe MK, Chen S, Zhang S. Community environment and HIV/AIDS-related stigma in China. AIDS Educ Prev 2005; 17: 1-11.

9. Elechiguerra JL, Burt JL, Morones JR, Camacho-Bragado A, Gao X, Lara HH. Interaction of silver nanoparticles with HIV-1. J Nanobiotechnol 2005; 3:6.

10. Chen X and Schluesener HJ. Nanosilver: a nanoproduct in medical application. Toxicol Lett 2008; 176:1-12.

11. Asharani PV, Hande MP, Valiyaveettil S. Anti-proliferative activity of silver nanoparticles. BMC Cell Biol 2009; 10: 65.

12. Ernest V, George Priya Doss C, Muthiah A, Mukherjee A, Chandrasekaran N. Genotoxicity assessment of low concentration AgNPs to human peripheral blood lymphocytes. Int J Pharm Pharm Sci 2013; 5: 377-381.

13. Wong K.K., Cheung S.O., Huang L. Further evidence of the anti-inflammatory effects of silver nanoparticles. Chem Med Chem. 2009; 4(7):1129–1135.

14. Kim, S.; Choi, J.E.; Choi, J.; Chung, K.H.; Park, K.; Yi, J.; Ryu, D.Y. Oxidative stress-dependent toxicity of silver nanoparticles in human hepatoma cells. Toxicol. In Vitro 2009; 23: 1076–1084.

15. Tang J, Xiong L, Wang S, Wang J, Liu L, Li J, et al.. Distribution, translocation and accumulation of silver nanoparticles in rats. J Nanosci Nanotechnol 2009; 9:4924–32.

16. García-Alonso J, Farhan R. Khan, Superb K. Misra, Mark Turmaine,| Brian D. Smith, Philip S. Rainbow, Samuel N. Luoma, and Valsami-Jones E (2011). Cellular Internalization of Silver Nanoparticles in Gut Epithelia of the Estuarine Polychaete Nereis diversicolor Environ. Sci. Technol 2011; 45: 4630–4636

17. Lee TY, Liu MS, Huang LJ, Lue SI, Lin LC, Kwan AL, Yang RC. Bioenergetic failure correlates with autophagy and apoptosis in rat liver following silver nanoparticle intraperitoneal administration. Part Fibre Toxicol 2013; 10: 40.

18. Kim YS, Kim JS, Cho HS, Rha DS, Kim JM, Park JD, Choi BS, Lim R, Chang HK, Chung YH, Kwon IH, Jeong J, Han BS and Yu IJ: Twenty-eight-day oral toxicity, genotoxicity, and gender-related tissue distribution of silver nanoparticles in Sprague–Dawley rats. Inhal Toxicol 2008; 20:575–583.

19. Kim, J S, Sung, J H, Ji JH, Song K.S., Lee JH, Kang CS, Yu IJ. In vivo genotoxicity of silver nanoparticles after 90 day silver nanoparticle inhalation exposure. Saf. Health Work 2011; 2: 65–69.

20. Asharani, P. V., Wu, Y. L., Gong, Z., et al.. Toxicity of silver nanoparticles in zebra fish models. Nanotechnology 2008; 19 (25):

255102.

21. Asharani P. V., Lianwu Y., Gong Z., Valiyaveettil S. Comparison of the toxicity of silver, gold and platinum nanoparticles in developing zebrafish embryos. Nanotoxicology 2011; 5:43–54.

22. Li W.-R., Xie X.-B., Shi Q.S., Duan S.S., Ou-Yang Y.-S., Chen Y.-B. Antibacterial effect of silver nanoparticles on Staphylococcus aureus. Biometals, 2011; 24: 135–141

23. Li F, Weir MD, Chen J, Xu HH. Comparison of quaternary ammonium-containing with nano-silver-containing adhesive in antibacterial properties and cytotoxicity. Dent. Mater.2013; 29(4):450-461.

24. El Mahdya M.M, Salah Eldinb T.A, Alyd H.S, Mohammed F.F, Shaalan M.I. Evaluation of hepatotoxic and genotoxic potential of silver nanoparticles in albino rats. Experimental and Toxicologic Pathology 2014; 67: 21–29

25. Patlolla A.K, Hackett D and Tchounwou P. Genotoxicity study of silver nanoparticles in bone marrow cells of Sprague-Dawley rats. Food Chem Toxicol. 2015; 85:52-60.

26. Ordzhonikidze CG, Ramaiyya LK, Egorova EM, Rubanovich AV. Genotoxic effects of silver nanoparticles on mice in vivo. Acta Naturae 2009; 1:99–101.

27. Tiwari DK, Jin T and Behari J. Dose-dependent in vivo toxicity assessment of silver nanoparticle in Wistar rats. Toxicol Mech Methods 2011; 21: 13-24.

28. Mohamed H.R.H . "Studies on the Genotoxicity Behavior of Silver Nanoparticles in the Presence of Heavy Metal Cadmium Chloride in Mice," Journal of Nanomaterials 2016; 2016, Article ID 5283162, 12 pages

29. Choi JE, Kim S, Ahn JH, Youn P, Kang JS, Park K, Yi J and Ryu DY. Induction of oxidative stress and apoptosis by silver nanoparticles in the liver of adult zebrafi sh. Aquat Toxicol 2010; 100:151-9.

30. Ahamed M, Posgai R, Gorey TJ, Nielsen M, Hussain SM and Rowe JJ. Silver nanoparticles induced heat shock protein 70, oxidative stress and apoptosis in Drosophila melanogaster. Toxicol Appl Pharmacol 2010; 242:263-9.

31. Laban, G., Nies, L.F., Turco, R.F., Bickham, J.W. and Sepúlveda, M.S.. The effects of silver nanoparticles on fathead minnow (Pimephales promelas) embryos. Ecotoxicology 2010; 19: 1 – 11

32. Li, P.W., Kuo, T.H., Chang, J.H., Yeh, J.M. and Chan, W.H.. Induction of cytotoxicity and apoptosis in mouse blastocysts by silver nanoparticles. Toxicology Letters 2010; 2: 82 –87.

33. Philbrook, N.A., Winn, L.M., Afrooz, A.R., Saleh, N.B. and Walker, V.K.. The effect of TiO (2) and Nano-Agon reproduction and development of Drosophila melanogaster and CD-1 mice. Toxicology and Applied Pharmacology 2011; 257: 429 – 436.

34. Attia A.A. Evaluation of the Testicular Alterations Induced By Silver Nanoparticles in Male Mice: Biochemical, Histological and Ultrastructural Studies. Research Journal of Pharmaceutical, Biological and Chemical Sciences 2014; 4: 1558- 1589

35. Gromadzka-Ostrowska, J., Dziendzikowska, K., Lankoff, A., Dobrzyoska, M., Instanes, C., Brunborg, G. et al.: Silver Nanoparticles effects on epididymal sperm in rats. Toxicol Lett. 2014; 214: 251 - 258.

36. Chuang S. M., Wang I. C. and Yang J. L.. Roles of JNK, p38 and ERK mitogen-activated protein kinases in the growth inhibition and apoptosis induced by cadmium. Carcinogenesis 2000; 21: 1423–1432.

37. Kim S., Moon C., Eun S., Ryu P. and Jo S.. Identification of ASK1, MKK4, JNK, c-Jun, and caspase-3 as a signaling cascade involved in cadmium-induced neuronal cell apoptosis. Biochem. Biophys. Res. Commun. 2005; 328: 326–334.

38. Robinson JF, Yu X, Moreira EG, Hong S, and Faustman EM.. Arsenic- and cadmiuminduced toxicogenomic response in mouse embryos undergoing neurulation. Toxicol Appl Pharmacol 2011;

250:117-129.

39. Lau A., Zhang J. and Chiu J. Acquired tolerance in cadmium adapted lung epithelial cells: roles of the c-Jun N-terminal kinase signaling pathway and basal level of metallothionein. Toxicol. Appl. Pharmacol. 2006; 215, 1–8.

40. Lopez E., Figueroa S., Oset-Gasque M. and Gonzalez M. P.. Apoptosis and necrosis: two distinct events induced by cadmium in cortical neurons in culture. Br. J. Pharmacol. 2003; 138: 901–911.

41. Celik A, B¨uy¨ukakilli B, Cimen B, Tasdelen B, Ozturk M.I, and Eke, D. Assessment of cadmium genotoxicity in peripheral blood and bone marrow tissues of maleWistar rats, *Toxicology Mechanism and Methods* 2009; 19(2): 135–140

42. Cambier S, Gonzalez P, Durrieu G, and Bourdineaud J-P. Cadmium-induced genotoxicity in zebrafish at environmentally relevant doses. Ecotoxicology and Environmental Safety 2010; 73(3): 312–319.

43. Abrahim K. S., Abdel-Gawad N. B., Mahmoud A. M, El- Gowaily M. M, Emara A. M, and Hwaihy M.M. Genotoxic effect of occupational exposure to cadmium," *Toxicology and Industrial Health* 2011; 27(2): 173–179.

44. Ali T. H. . "Determination of the lethal dose 50% (LD50) of cadmium chloride and the histopathological changes in male mice liver and kidneys" Journal of Education and Science 2012; 25(3):. 27–38

45. Tice R.R., Agurell E., Anderson V, Burlinson B., Hartmann A., Kobayashi H., Miyamae Y., Rojas E., Ryu J.C. and Sasaki Y.F.. Single cell gel/comet assay: guidelines for in vitro and in vivo genetic toxicology testing, Environ. Mol. Mutagen. 2000; 35: 206–221.

46. Kizilian N, R.C. Wilkins, P. Reinhardt, C. Ferrarotto, J.R.N. McLean, J.P. Mc- Namee. Silver-stained comet assay for detection of apoptosis. Biotechniques 1999; 27: 926–929.

47. Attia S.M., S.A. Al-Bakheet, N.M. Al-Rasheed. Proanthocyanidins produce significant attenuation of doxorubicin-induced mutagenicity via suppression of oxidative stress. Oxid. Med. Cell Longev 2010; 3(6): 404–413.

48. Sriram MI, Kanth SB, Kalishwaralal K ,Gurunathan S. Antitumor activity of silver nanoparticles in Dalton's lymphoma ascites tumor model. Int J Nanomedicine 2010; 5: 753-762.

49. Gutierrez, M. I., Bhatia, K., Siwarski, D., Wolff, L., Magrath, I. T., Mushinski, J. F. and Huppi1, K. Infrequent p53 mutation in mouse tumors with deregulated myc. *Cancer Res.*1992; 52, 1032–1035.

50. Gautheron V., A. Auffret, M. P. Mattson, J. Mariani, and B. Vernet-der Garabedian. "A new and simple approach for genotyping Alzheimer's disease presenilin-1 mutant knock-in mice," Journal of Neuroscience Methods 2009; 181(2): 235–240

51. Ohkawa, H., Ohishi, N. and Yagi, K. Assay for lipid peroxides in animal tissues by thiobarbituric acid reaction. Analytical Biochemistry 1979; 95: 351 – 358.

52. Beutler, E., O. Duron and B.M. Kelly. Improved method for the determination of blood glutathione. J. Lab. Clin. Med. 1963; 61: 882-888.

53. Nishikimi, M., Roa, N. A. and Yogi, K. Measurement of superoxide dismutase. Biochem. Biophys. Res. Commun. 1972; 46, 849–854.

54. Paglia, D. E. and Valentine, W. N. Studies on the quantitative and qualitative characterization of erythrocyte glutathione peroxidase. *J. Lab. Clin. Med.* 1967; 70, 158–169.

55. Jarup L, Berglund M, Elinder CG, Nordberg G, Vahter M. Health effects of cadmium exposure–a review of the literature and a risk estimate. Scand J Work Environ Health. 1998; 24:1–51.

56. Jarup L and Akesson A. Current status of cadmium as an environmental health problem. Toxicol Appl Pharmacol. 2009; 238:201–8.

57. Genter M.B, Newman N.C, H.G Shertzer, Ali S.F and Bolon B. Distribution and Systemic Effects of Intranasally Administered 25 nm Silver Nanoparticles in Adult Mice. Toxicologic Pathology 2009; 40: 1004-1013

58. Guo H, Zhang J, Boudreau M, Meng J, Yin J-j, Liu J and Xu H. Intravenous administration of silver nanoparticles causes organ toxicity through intracellular ROS-related loss of inter-endothelial junction. *Particle and Fibre Toxicology* 2016; 2016: 13:21

59. Valverde M, Fortoul T. I, Dias-Barriga F, Mejia J and del Castillo E. R. Induction of genotoxicity by cadmium chloride inhalation in several organs of CD-1 mice. Mutagenesis 2000; 15(2): 109-114

60. Błasiak J. P. DNA-Damaging Effect of Cadmium and Protective Action of Quercetin Journal of Environmental Studies 2001; 10(6): 437-442

61. Nava-Hernández MP[1], Hauad-Marroquín LA, Bassol-Mayagoitia S, García-Arenas G, Mercado-Hernández R, Echávarri-Guzmán MA, Cerda-Flores RM. Lead-, cadmium-, and arsenic-induced DNA damage in rat germinal cells. DNA Cell Biol. 2009 May; 28(5): 241-8.

62. Woodbine, L., Brunton, H., Goodarzi, A. A., Shibata, A. and Jeggo, P. A. Endogenously induced DNA double strand breaks arise in heterochromatic DNA regions and require ataxia telangiectasia mutated and Artemis for their repair. Nucleic Acids Res 2011; 39, 6986– 6997.

63. Casalino, E.; Sblano, C. and Landriscina, C. Enzyme activity alteration by cadmium administration to rats: The possibility of iron involvement in lipid peroxidation. Arch. Biochem. Biophys. 1997; *346*, 171–179.

64. Yang, J.M.; Arnush, M.; Chen, Q.Y.; Wu, X.D.; Pang, B. and Jiang, X.Z. Cadmium-induced damage to primary cultures of rat Leydig cells. *Reprod. Toxicol* 2003; *17*: 553–560.

65. Lips K and Kaina B. DNA-double stranded breaks trigger apoptosis in p53 deficient-fibroblasts. Carcinogenesis 2001; 22(4): 579-584

66. Tounekti1 O, Kenani1 A, Foray N, Orlowski S and Mir LM .The ratio of single- to double-strand DNA breaks and their absolute values determine cell death pathway. British Journal of Cancer (2001) 84(9), 1272–1279

67. Norbury C.J and Zhivotovsky B. DNA damage-induced apoptosis. Oncogene 2004; 23: 2797–2808

68. Jackson SP and Bartek J: The DNA-damage response in human biology and disease. Nature 2009; 461(7267):1071-1078.

69. Obe J, Johannes C and Schulte-Frohlinde D. DNA double-strands induced by sparsely ionizing radiation and endonucleases as a critical lesion for cell death, chromosomal aberrations, mutations and oncogenic transformation. Int. J. Radiat. Biol. 1992; 70: 199-208

70. Kaina B. Critical steps in alkylation-induced aberration formation. Mut. Res. 1998; 404: 119-124

71. Nilsberth C, Luthman J, Lannfelt L, Schultzberg M. Expression of presenilin-1 mRNA in rat peripheral organs and brain. Histochem J. Aug 1999; 31(8):515-23.

72. Van Ess PJ, Pedersen WA, Culmsee C, Mattson ' MP, Blouin R A. Elevated hepatic and depressed renal cytochrome P450 activity in the Tg2576 transgenic mouse model of Alzheimer's disease. Journal of Neurochemistry 2002; 80, 571-578

73. Das I, Craig C, Funahashi Y, Jung KM, Kim TW, Byers R, Weng AP, Kutok JL, Aster JC, Kitajewski J. Notch oncoproteins depend on gamma-secretase/presenilin activity for processing and function. J Biol Chem 2004; 279:30771–30780.

74. Fraering PC. Structural and Functional Determinants of gamma-Secretase, an Intramembrane Protease Implicated in Alzheimer's Disease. Curr Genomics 2007; 8:531–549.

75. Boulton ME, Cai J, Grant MB. gamma-Secretase: a multifaceted regulator of angiogenesis. J Cell Mol Med 2008; 12:781–795.

76. Rahimi N, Golde TE, Meyer RD. Identification of ligand-induced proteolytic cleavage and ectodomain shedding of VEGFR-1/FLT1 in leukemic cancer cells. Cancer research 2009; 69:2607–2614.

77. Cacquevel M, Aeschbach L, Houacine J, Fraering PC. Alzheimer's Disease-Linked Mutations in Presenilin-1 Result in a Drastic Loss of Activity in Purified c-Secretase Complexes. PLoS ONE 2012; 7(4): e35133.

78. Ohyagi Y, Asahara H, Chui DH, Tsuruta Y, Sakae N, Miyoshi K, Yamada T, Kikuchi H, Taniwaki T, Murai H, Ikezoe K, Furuya H, Kawarabayashi T, Shoji M, Checler F, Iwaki T, Makifuchi TT, Takeda K, Kira J, Tabira T. Intracellular Abeta42 activates p53 promoter: a pathway to neurodegeneration in Alzheimer's disease. FASEB J 2005; 19: 255-257.

79. Ma L, Ohyagi Y, Miyoshi K, Sakae N, Motomura K, Taniwaki T, Furuya H, Takeda K, Tabira T, Kira J. Increase in p53 protein levels by presenilin-1 gene mutations and its inhibition by secretase inhibitors. J Alzheimers Dis.2009; 16(3):565-75.

80. Dorszewska J, Oczkowska A, Suwalska M, Rozycka A, Florczak-Wyspianska J, Dezor M, Lianeri M, Jagodzinski P, Kowalczyk M.J, Prendecki M, Kozubski W. Mutations in the exon 7 of *Trp53* gene and the level of p53 protein in double transgenic mouse model of Alzheimer's disease. Folia Neuropathol 2014; 52 (1): 30-40.